AMERICAN SOCIETY FOR MICROBIOLOGY | Antimicrobial Agents and Chemotherapy®

EXPERIMENTAL THERAPEUTICS

A Low-Molecular-Weight Alginate Oligosaccharide Disrupts Pseudomonal Microcolony Formation and Enhances Antibiotic Effectiveness

Manon F. Pritchard,[a] Lydia C. Powell,[a] Alison A. Jack,[a]* Kate Powell,[a] Konrad Beck,[a] Hannah Florance,[b]* Julian Forton,[c] Philip D. Rye,[d] Arne Dessen,[d] Katja E. Hill,[a] David W. Thomas[a]

Advanced Therapies Group, Cardiff University School of Dentistry, Cardiff, United Kingdom[a]; Department of Biosciences, College of Life and Environmental Sciences, Exeter University, Exeter, United Kingdom[b]; Childrens Hospital of Wales, Paediatric Respiratory Medicine, Cardiff, United Kingdom[c]; AlgiPharma AS, Sandvika, Norway[d]

ABSTRACT In chronic respiratory disease, the formation of dense, 3-dimensional "microcolonies" by *Pseudomonas aeruginosa* within the airway plays an important role in contributing to resistance to treatment. An *in vitro* biofilm model of pseudomonal microcolony formation using artificial-sputum (AS) medium was established to study the effects of low-molecular-weight alginate oligomers (OligoG CF-5/20) on pseudomonal growth, microcolony formation, and the efficacy of colistin. The studies employed clinical cystic fibrosis (CF) isolates ($n = 3$) and reference nonmucoid and mucoid multidrug-resistant (MDR) CF isolates ($n = 7$). Bacterial growth and biofilm development and disruption were studied using cell viability assays and image analysis with scanning electron and confocal laser scanning microscopy. Pseudomonal growth in AS medium was associated with increased ATP production ($P < 0.05$) and the formation (at 48 h) of discrete (>10-μm) microcolonies. In conventional growth medium, colistin retained an ability to inhibit growth of planktonic bacteria, although the MIC was increased (0.1 to 0.4 μg/ml) in AS medium compared to Mueller-Hinton (MH) medium. In contrast, in an established-biofilm model in AS medium, the efficacy of colistin was decreased. OligoG CF-5/20 (≥2%) treatment, however, induced dose-dependent biofilm disruption ($P < 0.05$) and led to colistin retaining its antimicrobial activity ($P < 0.05$). While circular dichroism indicated that OligoG CF-5/20 did not change the orientation of the alginate carboxyl groups, mass spectrometry demonstrated that the oligomers induced dose-dependent (>0.2%; $P < 0.05$) reductions in pseudomonal quorum-sensing signaling. These findings reinforce the potential clinical significance of microcolony formation in the CF lung and highlight a novel approach to treat MDR pseudomonal infections.

KEYWORDS *Pseudomonas aeruginosa*, colistin, cystic fibrosis, alginate, OligoG CF-5/20

Received 19 April 2017 **Returned for modification** 15 May 2017 **Accepted** 6 June 2017

Accepted manuscript posted online 19 June 2017

Citation Pritchard MF, Powell LC, Jack AA, Powell K, Beck K, Florance H, Forton J, Rye PD, Dessen A, Hill KE, Thomas DW. 2017. A low-molecular-weight alginate oligosaccharide disrupts pseudomonal microcolony formation and enhances antibiotic effectiveness. Antimicrob Agents Chemother 61:e00762-17. https://doi.org/10.1128/AAC.00762-17.

Address correspondence to Manon F. Pritchard, pritchardmf@cardiff.ac.uk.

* Present address: Alison A. Jack, Cultech Limited, Port Talbot, United Kingdom; Hannah Florance, UK Centre for Mammalian Synthetic Biology, Edinburgh, United Kingdom.

The opportunistic Gram-negative pathogen *Pseudomonas aeruginosa* is found in a range of chronic human respiratory diseases, including chronic obstructive pulmonary disease and cystic fibrosis (CF) (1). CF is a life-threatening, autosomal recessive genetic disorder affecting 1 in 2,300 Caucasian live births (2). Reduced airway surface-liquid volume and abnormally viscous sputum result in ineffective mucociliary clearance (3). Chronic bacterial colonization of the lung by a number of opportunist pathogens occurs, most notably *P. aeruginosa*, which predominates with time (4).

Within the diseased lung, pathoadaptive mutation results in the selection of hypermutator *P. aeruginosa* strains (5, 6). In *P. aeruginosa*, this adaption occurs with a switch to the mucoid phenotype, characterized by overproduction of high-molecular-mass

(>15-kDa) alginate exopolysaccharide (EPS) (7, 8). This switch is accompanied by modification of acyl homoserine lactone (AHL)- and *Pseudomonas* quinolone signal (PQS)-dependent quorum-sensing (QS) systems (9), with altered production of virulence factors, e.g., pyocyanin and hydrogen cyanide (10). Extracellular alginate affords protection from host innate immune responses, including phagocytosis and neutrophil-derived reactive oxygen species (11). Mucoidal pseudomonal strains are often unresponsive to aggressive antibiotic selection (12), and 18.1% of CF patients are colonized with multidrug-resistant (MDR) *P. aeruginosa* (13).

In contrast to standard laboratory models of bacterial biofilm formation on material surfaces, biofilms within the CF lung form as nonadherent spherical microcolonies embedded in respiratory mucin (14, 15). While *in vitro* studies of *P. aeruginosa* from CF lungs routinely employ nutrient-rich media to optimize bacterial growth or Mueller-Hinton (MH) medium, such media fail to adequately reproduce the lung environment or secretome (3). More recently, defined media, such as artificial-sputum (AS) medium (containing components of CF sputum, e.g., DNA, mucin, mineral salts, proteins, and amino acids), have been employed to model the behavior of *P. aeruginosa* (16–18). These AS medium models have been used to study the adaptation of pathogens to the CF lung using whole-genome sequencing and microarray expression profiling (19), to analyze diffusion (20), and to test the effectiveness of antibacterial therapeutics (21).

The distinctive biofilm microcolony formation in the CF lung has been demonstrated *ex vivo* in freshly excised intraluminal material and in lung sections (14). Studies have further shown that *in vitro* biofilms observed under nutrient-limited conditions are increasingly recalcitrant to antibiotic therapy due to enhanced tolerance (22). The design and delivery of antimicrobial therapy targeted against the polymicrobial respiratory biofilm is, therefore, challenging (23).

The acquisition of MDR *Pseudomonas* in the CF lung has led to a resurgence of clinical interest in the bactericidal antibiotic colistin (24). Overlooked for many years due to associated nephro- and neurotoxicity (25, 26), colistin is increasingly used to treat life-threatening infections (24) and as an inhaled therapy in CF to prevent establishment of infection by MDR bacteria (25). While resistance to colistin remains low (27), the emergence of colistin-resistant strains heralds fears of a postantibiotic era (28).

We previously described the use of a low-molecular-weight alginate oligomer (OligoG CF-5/20; ≥85% guluronic acid, with a degree of polymerization [DPn] of 16; number average molecular weight [Mn], 3,200) from the seaweed *Laminaria hyperborea* as a promising novel therapy in CF (29–31). *In vitro* studies demonstrated the ability of OligoG CF-5/20 to modify the bacterial surface charge (30) and biofilm growth of nonmucoid *Pseudomonas* spp. in conventional culture/biofilm models (29). It is, however, important to determine whether OligoG CF-5/20 can modify bacterial growth within the inherently antibiotic-resistant microcolonies that characterize the diseased CF lung.

The objective of this study was to investigate the therapeutic efficacy of OligoG CF-5/20 and colistin in an *in vitro* microcolony model. We characterized the growth of fresh clinical isolates from CF patients and strains from the International *P. aeruginosa* Reference Panel (IPARP). Planktonic and biofilm cultures of wild-type PAO1 and the mucoid NH57388A were studied in MH and AS media. We developed microcolonies in the AS medium, investigated the ability of OligoG CF-5/20 to modify these biofilms, and, further, determined the effectiveness of a combination treatment with colistin. The effect of colistin treatment alone, on the mucoid CF isolate NH57388A grown under planktonic and biofilm conditions, was reduced in this AS medium. In contrast, OligoG CF-5/20 demonstrated a dose-dependent antibiofilm effect, as well as retaining the effectiveness of colistin *in vitro*, demonstrating that addition of alginate oligosaccharides modifies pseudomonal microcolony assembly.

RESULTS

Nonmucoid *P. aeruginosa* IPARP strains have higher growth rates in MH medium than either mucoid or new nonmucoid CF isolates. Growth of nonmucoid *P. aeruginosa* from the IPARP reference strains in MH medium was more abundant (maximum absorbance, ≥1) than the delayed, weaker growth of the fresh clinical isolates (maximum absorbance, ≤1), reaching stationary phase at 12 h versus 20 h, respectively (Fig. 1A). However, SpIT22554 reached a yield similar to that of the IPARP reference strains at 24 h. The growth rates of the nonmucoid *P. aeruginosa* strains (PAO1, AA2, and AA44) were also higher than those of the new CF isolates (22476, 22078, and 22554) and most mucoidal strains (IST27, 2192, and NH57388A) from the IPARP collection (Fig. 1B), with doubling times (at maximum exponential growth) of 0.2 to 0.23 versus 0.31 to 0.6 versus 0.29 to 0.56 unit/h, respectively.

Colistin retains its antimicrobial properties in the presence of the mucolytic OligoG CF-5/20. Initial studies on the effects of OligoG CF-5/20 and colistin (0.5× MIC) on pseudomonal growth in MH medium demonstrated no difference between the growth rate of NH57388A when treated with colistin (0.16 unit/h) and that of the control (Fig. 1C), although a reduced growth rate (0.12 unit/h) was noted when it was exposed to either 2% OligoG CF-5/20 or colistin with 2% OligoG CF-5/20. This was reflected in the significantly decreased cell biomass at stationary phase (36 h) following treatment with 2% OligoG CF-5/20 in combination with colistin compared to that of the control ($P < 0.05$).

In the biofilm disruption assay, confocal laser scanning microscopy (CLSM) images of LIVE/DEAD-stained, 24-h established pseudomonal biofilms demonstrated homogeneous growth in the untreated control (Fig. 1D). Treatment for 1 h with colistin alone at 0.5× the minimum biofilm eradication concentration (MBEC), as previously described (32), was associated with decreased density of the resultant biofilm (Fig. 1E). Furthermore, when treated with 2% OligoG CF-5/20 alone for 1 h, the biofilm height was reduced and there was increased porosity (Fig. 1F). Combination treatment with colistin and 2% OligoG CF-5/20 resulted in marked biofilm disruption (Fig. 1G). Quantification using COMSTAT image analysis software (33) revealed that biofilm height was significantly reduced, from 11 ± 4 μm (in the untreated control) to 1.1 ± 0.2 μm, following 2% OligoG CF-5/20 and colistin combination treatment (Fig. 1H). In parallel, the ratio of dead to live cells was significantly increased following exposure to colistin (0.24 ± 0.07) or 2% OligoG CF-5/20 and colistin in combination (0.49 ± 0.22) compared to the control (0.053 ± 0.014; $P < 0.05$) (Fig. 1I), with associated increases in porosity. A significant reduction in biofilm biomass was obtained following 2% OligoG CF-5/20 treatment with or without colistin (Fig. 1J), with a corresponding trend toward increased surface roughness (Fig. 1K).

Mucoid and nonmucoid *P. aeruginosa* strains show a distinctly altered biofilm phenotype in artificial-sputum medium. Biofilms grown in different nutrient media exhibited distinct patterns of growth, with a marked phenotypic difference in biofilm architecture in MH versus AS medium (Fig. 2A and B). Pseudomonal biofilms of both strains showed conventional homogeneous growth in MH medium, while discrete, spherical microcolonies were apparent in AS medium. The microcolonies were not strongly bound to the well plates and varied considerably in size. The median diameters of the PAO1 and NH57388A microcolonies were 14 ± 4 μm and 11 ± 5 μm, respectively, with the difference in size perhaps reflecting the lower growth rate of the mucoid strain. Elongated structures between the microcolonies were composed of linearly arranged bacterial cells.

Growth curves were performed using a cell viability assay (measuring ATP production), as conventional growth curves with optical-density measurements were impractical in AS medium, due to bacterial aggregation and microcolony formation. Marked differences in ATP production between cells grown in AS versus MH medium were evident within 24 h, and were considerably elevated in AS medium (Fig. 2C).

OligoG CF-5/20 disrupts *P. aeruginosa* (NH57388A) microcolony formation in artificial-sputum medium. Scanning electron microscopy (SEM) studies using a biofilm

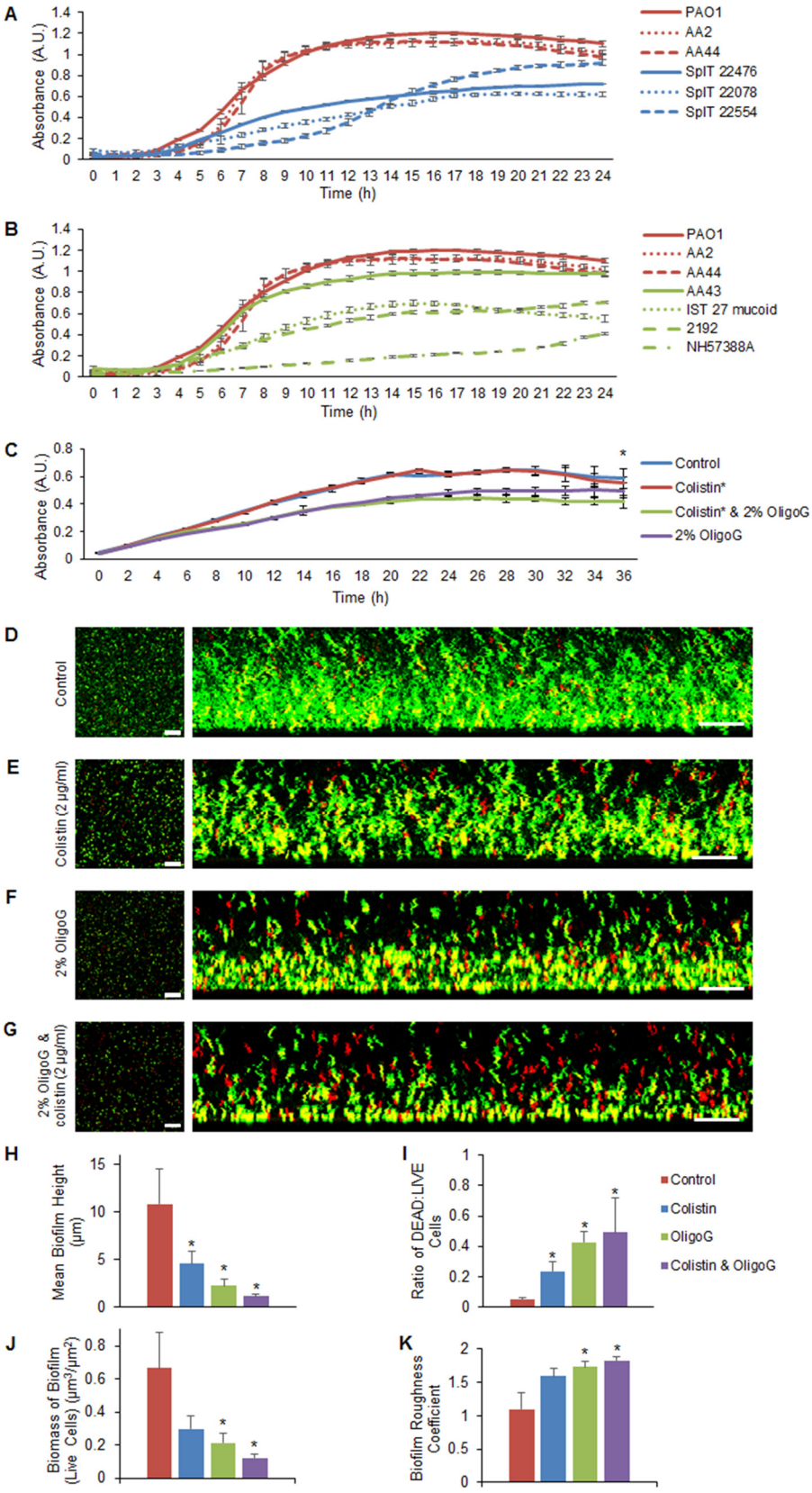

FIG 1 Comparison of planktonic growth in MH medium of characterized and new cystic fibrosis *P. aeruginosa* isolates and biofilm growth following antimicrobial treatment. (A and B) Growth curves (24 h) of nonmucoid IPARP isolates (red) versus fresh clinical SpIT isolates (blue) (A) and nonmucoid IPARP isolates (red) versus mucoid isolates (green) (B). A.U., arbitrary units. (C) Growth curves (±2%) of NH57388A (36 h)

(Continued on next page)

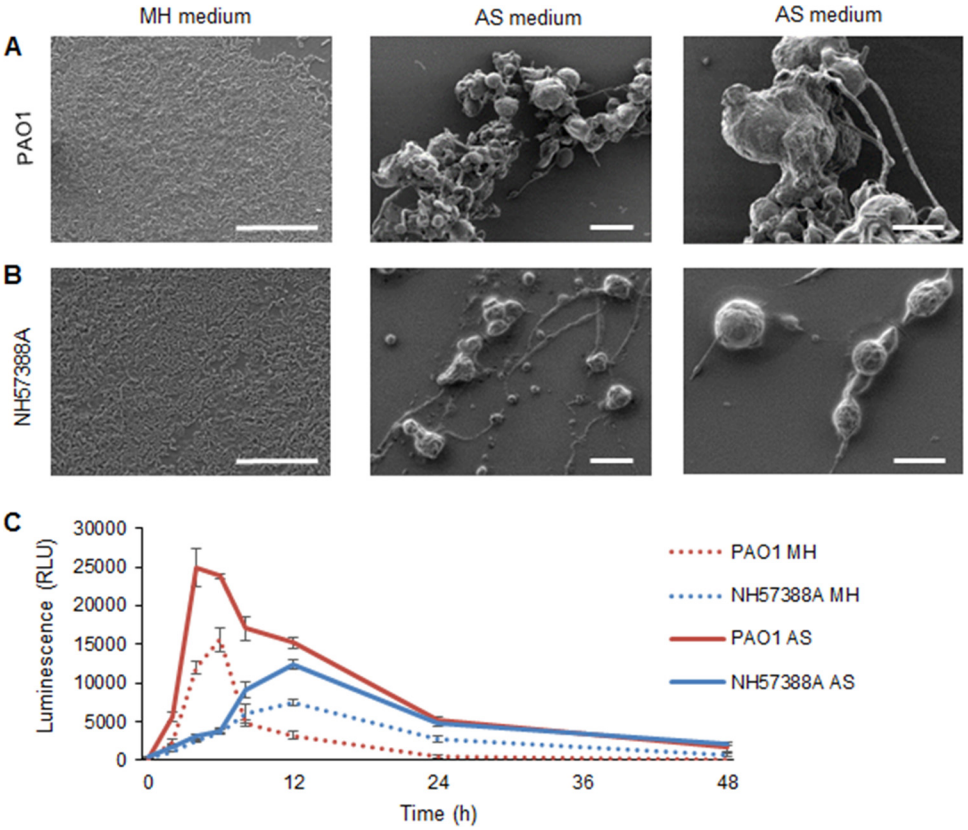

FIG 2 Comparison of growth of nonmucoid PAO1 and mucoid NH57388A *P. aeruginosa* in MH and AS media. (A and B) Scanning electron microscopy of bacterial growth in MH (24 h) and AS (48 h) media (scale bars, 20 μm), with corresponding enlarged images in AS medium (scale bars, 10 μm) (right). (A) PAO1. (B) NH57388A. (C) Cell viability (ATP production) of *P. aeruginosa* NH57388A and PAO1 (10^8 CFU/ml) grown in MH and AS media. RLU, relative light units. The error bars indicate standard deviations.

formation assay of *P. aeruginosa* (NH57388A) biofilms grown in MH medium with or without OligoG CF-5/20 demonstrated the growth-inhibitory effects of OligoG CF-5/20 at $\geq$2% (wt/vol) (Fig. 3A), which was reflected in a corresponding reduction in EPS formation. Mucoid *P. aeruginosa* (NH57388A) formed typical microcolonies in AS medium at 48 h (Fig. 3B); with individual bacterial cells visible on the surfaces of the microcolonies encased in EPS (Fig. 3C). Biofilm formation in the presence of OligoG CF-5/20 was associated with a dose-dependent decrease in microcolony size and increasing cellular disruption of the biofilms. At 6% OligoG CF-5/20, the median microcolony diameter was 4.5 μm versus 6.6 μm in the untreated control (Fig. 3D). Corresponding CLSM images of Syto-9 and concanavalin A 633 matrix-stained NH57388A 48-h biofilms in AS medium showed dense microcolonies surrounded by EPS (red) throughout the structure (Fig. 3E). Biofilms grown in OligoG CF-5/20 exhibited decreased overall biofilm mass with few spherical microcolonies and reduced EPS.

Using the biofilm disruption assay, CLSM images of matrix-stained NH57388A 48-h established biofilms stained with Syto-9 (green) demonstrated large cellular aggregates or microcolonies (Fig. 3F) on (or within) a layer of cells. Treatment for 1 h with 2% OligoG CF-5/20 induced a reduction in aggregate size (Fig. 3G), with marked micro-

FIG 1 Legend (Continued)
and OligoG CF-5/20 with or without colistin (0.05 μg/ml). (D to G) Biofilm disruption assay showing LIVE/DEAD CLSM (scale bars: aerial [left] and side views [right], 35 μm and 20 μm, respectively) of 24-h established NH57388A biofilms showing untreated control (D), 1-h colistin treatment (E), 2% OligoG CF-5/20 (F), and combined treatment (G). (H to K) COMSTAT analysis showing mean height of biofilm (H), ratio of dead to live cells (I), biomass of biofilm (J), and biofilm roughness coefficient (*K*) (*, $P < 0.05$). The error bars indicate standard deviations.

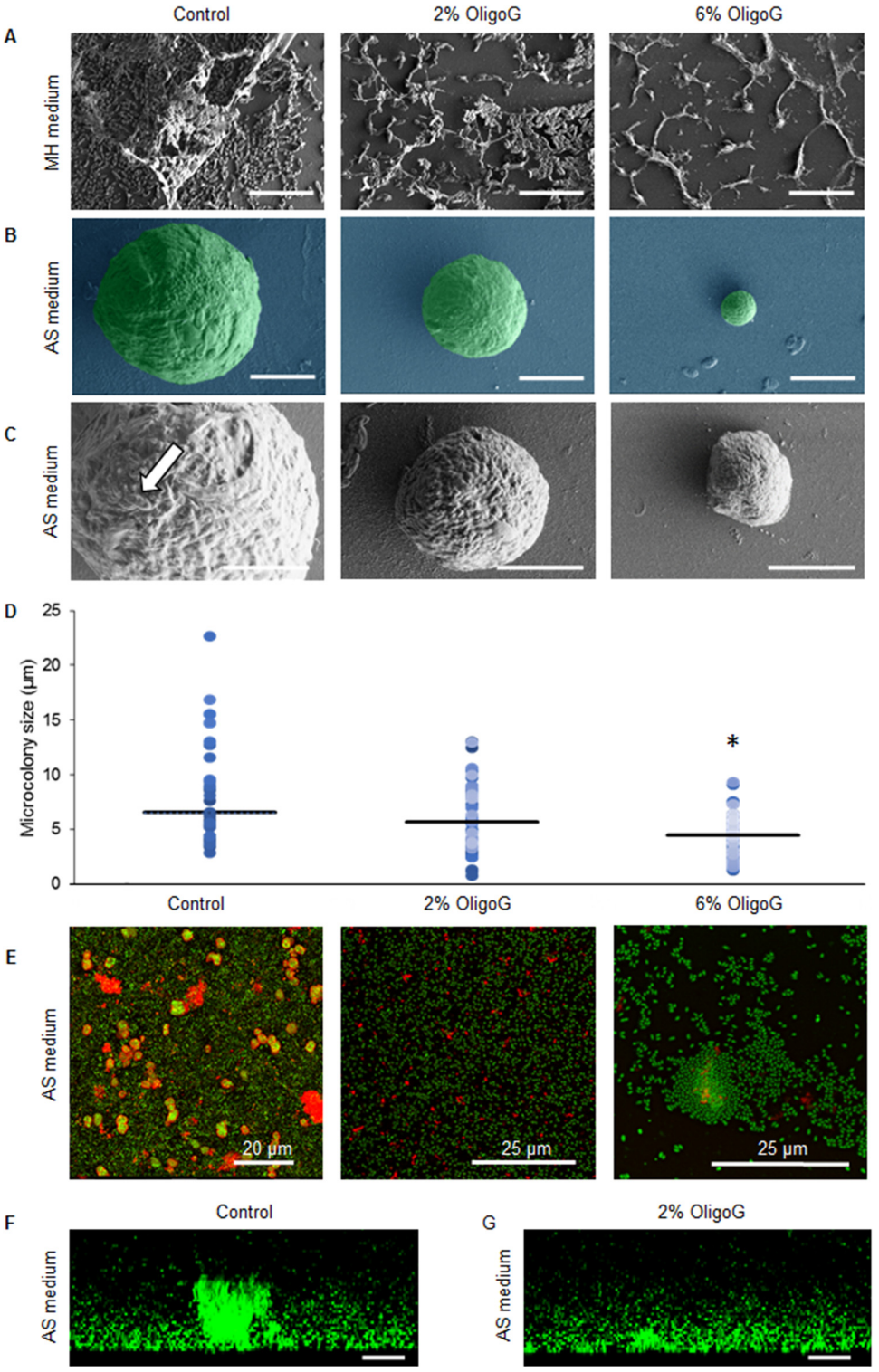

FIG 3 Biofilm formation assays showing mucoid *P. aeruginosa* NH57388A biofilms grown in MH and AS media. (A to D) SEM images of *P. aeruginosa* NH57388A biofilms grown with or without OligoG CF-5/20 for 24 h in MH medium (A) or for 48 h with or without OligoG CF-5/20 (scale bars, 5 μm) (B, enlarged in panel C; the arrow highlights individual cells) and corresponding scatter graphs showing approximate mean microcolony sizes (horizontal lines) (D). (E) Corresponding CLSM EPS staining of *P. aeruginosa* NH57388A 48-h biofilms in AS medium using Syto-9 (green) and concanavalin A 633 (red). (F and G) Biofilm disruption assay using Syto-9 (green) showing cross-sectional views of 48-h established biofilms treated for I h with 2% OligoG CF-5/20 (scale bars, 10 μm) (*, $P < 0.05$).

colony disruption. Three-dimensional (3D) videos of these images are available online (see Video S1 in the supplemental material).

Circular-dichroism spectra of OligoG CF-5/20 mixed with high-molecular-weight pseudomonal alginate do not indicate a specific interaction. Circular dichroism (CD) spectroscopy was used to test whether OligoG CF-5/20 and the high-molecular-weight EPS alginate produced by mucoid pseudomonal strains showed a specific interaction. The CD chromophore responsible for the Cotton effect observed at ca. 210 nm has been identified as the carboxyl groups of the alginates, and the $n \rightarrow \pi^*$ transition reflects their orientation (34). Upon heating from 4 to 37°C, spectra of high-M_w alginate showed no changes over a period of ~80 min (see Fig. S1, scans 1 to 7, in the supplemental material). Subsequent addition of OligoG CF-5/20 at a 50-fold molar excess resulted in an increased CD amplitude, i.e., more negative values (see Fig. S1, scans 8 to 11, in the supplemental material). Addition of Ca^{2+} to a final concentration of 1 mM had no effect (see Fig. S1, scans 12 to 17). The spectra observed for the high-M_w alginate–OligoG CF-5/20 mixture corresponded to an additive effect of the two components that did not indicate any change in the orientation of the carboxyl groups (dashed curves in Fig. S1). Experiments in which Ca^{2+} was added to the high-M_w alginate before the addition of OligoG CF-5/20, and a 1:600 molar ratio of high-M_w alginate to OligoG CF-5/20, also are compatible with an additive effect with no indication of a change in the orientation of the carboxyl groups (see Fig. S2 in the supplemental material).

OligoG CF-5/20 affects cell signaling in pseudomonal biofilms. To determine whether OligoG CF-5/20 effected these changes via modification of QS signaling in the biofilm systems, liquid chromatography-mass spectrometry (LC-MS) was employed to detect the pseudomonal signaling molecules, C_4- and 3-oxo-C_{12}-AHLs. AHL levels were determined at 30 and 48 h for PAO1 cells grown in both MH and AS media. Initial experiments compared growth in MH and AS media at 30 h (as at earlier time points in AS medium, AHLs were at the limits of detection [results not shown]). The LC-MS values indicated a reduction in the production of both 3-oxo-C_{12}-AHL and C_4-AHL signaling molecules in AS medium (62- and 783-fold, respectively) compared to MH medium (Fig. 4A). Further experiments were performed on OligoG CF-5/20-treated cultures grown in AS medium for 30 and 48 h (corresponding to mid- and late stationary phase, respectively). Interestingly, in this model, it was evident that OligoG CF-5/20 (0.2 to 2%) induced a dose-dependent decrease in 3-oxo-C_{12}-AHL (produced by the Las pathway) in comparison to the control at 30 and 48 h (Fig. 4B) but did not induce any significant change in C_4-AHL (produced by the RhlI pathway) (Fig. 4C). Although OligoG CF-5/20 had a significant effect on biofilm formation, there was no marked difference in ATP production (cell viability) by PAO1 or NH57388A following treatment (Fig. 4D and E).

The antibiotic properties of colistin were retained in artificial-sputum medium when combined with OligoG CF-5/20. Assays of biofilm disruption in established (24-h) nonmucoid (PAO1) and mucoid (NH57388A) pseudomonal biofilms following 24-h exposure to OligoG CF-5/20 and/or colistin were conducted in AS medium. The observed MIC value for colistin was 4 times greater in AS medium than in MH medium (0.4 μg/ml versus 0.1 μg/ml). The MIC employed in subsequent studies was based upon these findings.

As observed previously, PAO1 and NH57388A demonstrated the formation of large numbers of spherical microcolonies with extensive EPS in this model (Fig. 5A and B). The mucoidal NH57388A biofilms were characterized by microcolonies smaller than those of PAO1 (median diameter, 11 μm versus 14 μm, respectively) (Fig. 5C and D). Biofilm treatment with colistin at 4× the MBEC value (32) induced disruption of PAO1 and NH57388A bacterial networks. The microcolonies, however, remained intact (with no change in median diameter; $P > 0.05$). In contrast, treatment with 2% OligoG CF-5/20 induced significant decreases in the median microcolony diameter (6.9 ± 2.0 μm and 6.1 ± 2.7 μm for PAO1 and NH57388A, respectively; $P < 0.05$) characterized

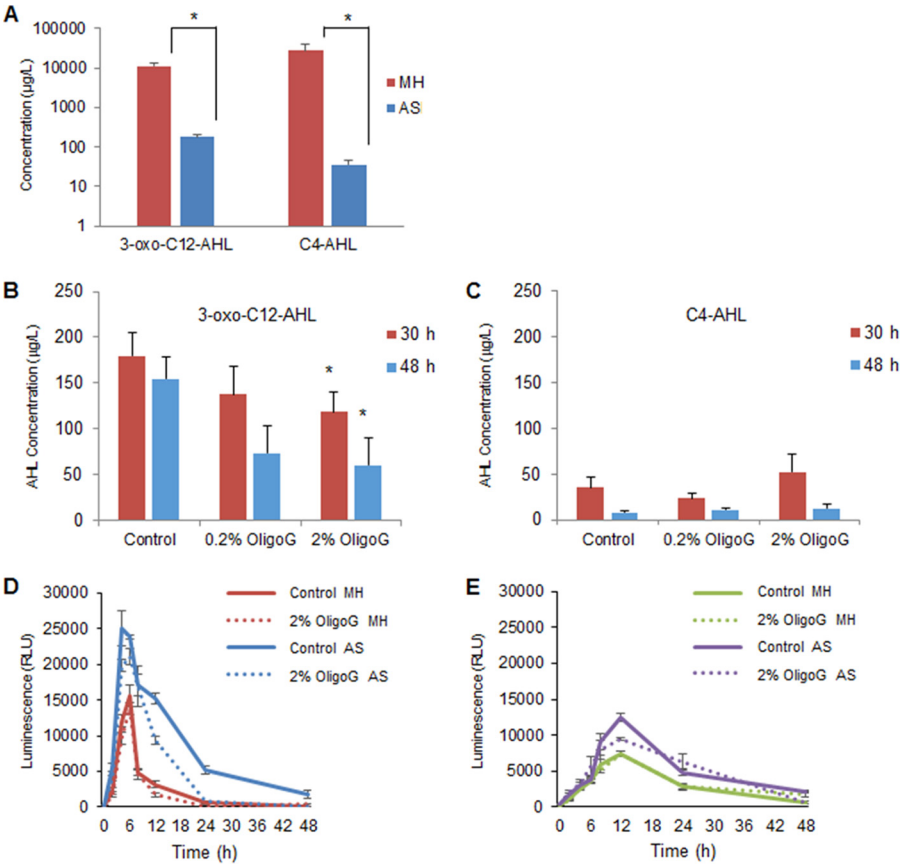

FIG 4 Effects of OligoG CF-5/20 on high-M_w alginate and on cell signaling molecules *in vitro*. (A to C) LC-QQQ-MS to quantify AHL (3-oxo-C_{12}-AHL and C_4-AHL) production by *P. aeruginosa* PAO1 grown in MH and AS media (30 h) (A) and in a time course assay (30 and 48 h) showing the effects of OligoG CF-5/20 on 3-oxo C_{12}-AHL (B) and C_4-AHL (C) (*, $P < 0.05$; $n = 3$). (D and E) Cell viability (ATP production) over 48 h of PAO1 (D) and NH57388A (E) grown in MH and AS media with or without 2% OligoG CF-5/20. The error bars indicate standard deviations.

by marked disruption of the intercolony networks and microcolony morphology. Combining OligoG CF-5/20 with colistin, although not as effective as OligoG CF-5/20 alone on the mucoid strain, effectively disrupted both microcolony structure (reducing the median diameter by 60% in PAO1) and the intercolony branching/bridging in both mucoid and nonmucoid models. The overall structural differences can be seen at a lower magnification in Fig. S3 in the supplemental material.

DISCUSSION

The improved survival of CF patients, due in part to the chronic administration of antibiotics, has compounded the problems associated with resistance to antibiotic treatment (35, 36). With the rapid emergence of antibiotic resistance, the development of new therapies is essential. Increased antibiotic resistance in biofilms has been extensively described, with biofilms shown to resist antibiotics by up to 1,000-fold (37). These studies demonstrate the potential benefits of combination therapies using a novel mucolytic alongside conventional antibiotics in the treatment of antibiotic-resistant, microcolony-forming *Pseudomonas* sp. lung infections.

The resurgence of interest in colistin, a highly effective membrane-permeabilizing antibiotic, reflects the failure of conventional antibiotics in MDR bacterial infections (25). Unfortunately, the emergence of plasmid-mediated colistin resistance provides the imminent possibility of horizontal gene transfer from veterinary to human pathogens (38). Due to the high rate of MDR in *P. aeruginosa* (39), colistin is now regarded as an antibiotic of last resort, and its use (in non-CF patients) is therefore limited to prevent further development of resistance (40).

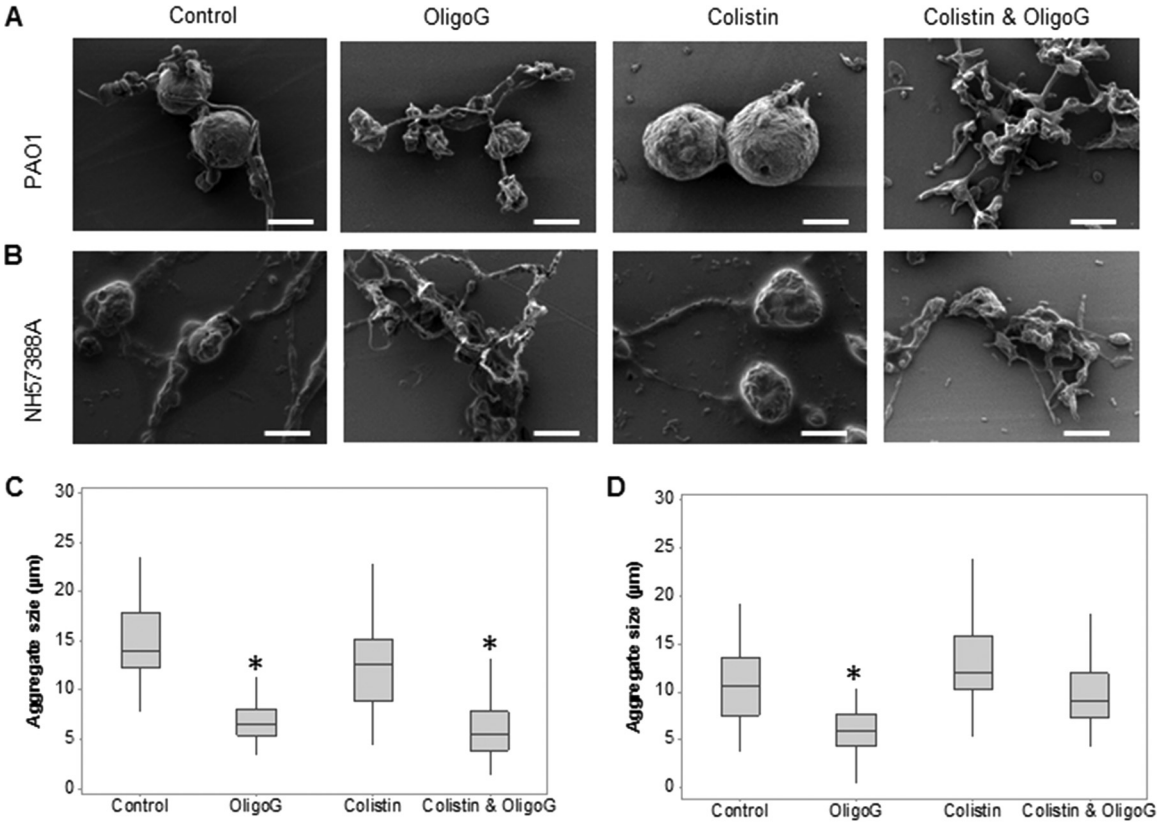

FIG 5 Biofilm disruption assays showing SEM of antimicrobial (OligoG CF 5/20 and colistin)-treated biofilms grown in AS medium (scale bars, 10 μm). Shown are SEM images of established (24-h) *P. aeruginosa* PAO1 (A) and NH57388A (B) biofilms exposed for 24 h to 2% OligoG CF-5/20 with or without colistin (16 μg/ml) with corresponding median microcolony diameter measurements for PAO1 (C) and NH57388A (D) (*, $P < 0.05$).

Colistin acts through positively charged electrostatic interactions with the negatively charged bacterial lipopolysaccharide (LPS), facilitating membrane disruption. The observed lowering of the efficacy of colistin in AS medium, therefore, may not only be related to an altered growth rate in this environment (which mimics growth conditions in the CF lung), but also may be due to LPS modification and/or direct binding by mucin in the AS medium, effectively sequestering free antibiotic (41). This EPS effect, and the apparent differences in MICs for colistin-treated NH57388A (with MIC values 4 times greater in AS than in MH medium) reflect the 10^4-fold difference previously observed between MIC (0.094 μg/ml) and MBEC (>512 μg/ml) values for NH57388A *in vitro* (32).

Within the diseased CF lung, >95% of *P. aeruginosa* bacteria exist in dense microcolonies >5 μm from the epithelial-cell surface and independent of cell surface attachment (14, 42). The microcolonies develop in the early stages of lung infection and readily resist physical disruption (42). The AS medium employed here induced pseudomonal microcolony formation in both nonmucoid and mucoid strains, as seen previously. The microcolonies resembled those observed in a range of CF epidemic and nonepidemic *P. aeruginosa* strains (16), with SEM demonstrating bridges between the microcolonies that appeared to be composed of elongated single cells encased in EPS, as previously observed in flow cell systems (43). OligoG CF-5/20 was able to modulate both the size and structure of these bacterial microcolonies. This may be related to its ability to interact with the EPS component of the biofilm by direct effects on the pseudomonal bacterial cell surface and on bacterial growth (29, 30). While imaging studies demonstrated that colistin effectively disrupted the intercolony bridges, the microcolonies (which were encased in EPS) appeared unaffected by colistin alone.

Despite the possible charge interactions between the cationic peptide colistin (41)

and the anionic OligoG CF-5/20 (30), colistin retained its antibiotic activity in the presence of OligoG CF-5/20. The ability of OligoG CF-5/20 to modify biofilm assembly in *Pseudomonas* spp. has previously been attributed to irreversible binding at the bacterial cell surface (30). Moreover, the ability of OligoG CF-5/20 to potentiate the effectiveness of colistin against mucoid NH57388A biofilms has recently been demonstrated in MBEC assays (32).

In this model, the ability of OligoG CF-5/20 (both alone and more markedly with colistin) to effectively disrupt the EPS of established biofilms was clearly evident. Disruption of the tight EPS network, which comprises >90% of the biofilm dry weight (44), has been shown to lead to less mechanically stable biofilms, which are then more susceptible to antibiotics (45). It appears, therefore, that during EPS disruption by OligoG CF-5/20, the antimicrobial action of colistin was retained by reducing its ability to bind to components of the biofilm matrix, thereby increasing its penetration through the biofilm, facilitating access of colistin to the pseudomonal cell membrane.

Initial experiments demonstrated the contrasting growth phenotype between freshly isolated clinical strains and the well-characterized reference strains. Compensatory mutations in the clinical CF isolates are thought to provide differential fitness benefits, which are advantageous within the CF lung environment (46). Fitness tradeoffs, where beneficial adaptations that improve fitness under one environmental condition that may lead to compensatory loss of other traits, have been described (47). This may, in part, explain the observed lower growth rate of fresh clinical isolates (adapted to the CF lung) compared to the laboratory-maintained IPARP CF strains. This variability highlights the importance of utilizing the reference strain collection for therapeutic development to ensure global standardization of *in vitro* testing.

A number of approaches have been attempted to modify biofilm EPS and facilitate treatment or displacement therapy. They have included use of bacterial polysaccharides, e.g., from marine *Vibrio* spp. (48); coadministration of alginate lyase with DNase, which has been reported to increase the efficacy of antibiotics in reducing biofilm growth (49); and coadministration of antibiotics with alginate lyase to eliminate mucoid variants not affected by antibiotics alone (50). Interestingly, we have also previously demonstrated synergy between OligoG CF-5/20 and recombinant human DNase I (rhDNase I) in modifying the mechanical and structural properties of CF sputum (31).

Biofilms also contain bacterially derived alginates that, in contrast to OligoG CF-5/20, lack G-blocks and have a considerably higher molecular mass (51). Anionic EPS components, such as carboxyl groups, interact strongly with multivalent cations, such as Ca^{2+}, resulting in robust biofilms (52). Sletmoen et al. (53) demonstrated that alginate oligomers may destabilize the interaction between high-M_w bacterially produced alginates and mucin. The ionic displacement of divalent cations, e.g., Ca^{2+}, has been described as a mechanism by which antimicrobial cationic peptides can potentiate antibiotics (54). Similarly, the anionic alginate G-blocks may displace divalent cations associated with the biofilm, resulting in a weaker biofilm structure. CD spectroscopy has previously been used to investigate the structural and conformational changes of polysaccharides containing uronic acid residues and has recently been employed to characterize homopolymeric fractions of the linear copolymers L-guluronate and D-mannuronate (34, 55). The gelation of alginate in the presence of divalent cations, such as Ca^{2+}, in homopolyguluronic acid is known to induce changes in the coordination of the carboxylate groups (56). However, CD spectra indicated that the orientation of the carboxy groups monitored at ~210 nm were not changed upon mixing OligoG CF-5/20 with high-M_w alginate.

Previous studies in planktonic systems demonstrated that OligoG CF-5/20 modified both *pilE* gene expression and bacterial motility in *P. aeruginosa* (30), which are controlled by QS. The finding that levels of *P. aeruginosa* AHL signaling molecules were significantly reduced in AS medium compared to MH medium was perhaps unsurprising, reflecting the change in growth/morphology. Sriramulu et al. (42) showed the importance of *lasR* for the formation of the dense-microcolony phenotype, and these data demonstrated the ability of ≥2% OligoG CF-5/20 to significantly reduce 3-oxo-C_{12}-AHL production

during both mid- and late-stationary-phase growth (30 and 48 h). The lack of an observed effect on the Rhl product, C_4-AHL, may reflect the reduced expression of *rhlR* that is known to occur in AS medium (16).

These experiments demonstrate that the previously described antibacterial effects of OligoG CF-5/20 are evident in this pseudomonal microcolony assay system, which more closely resembles growth in the CF lung. It must be remembered that many of the components of the *in vivo* lung are absent in the biofilm model, including lactoferrin, lipids, and oligopeptides, which may modulate bacterial behavior *in vivo*. OligoG CF-5/20 was shown to disrupt the biofilm EPS network, and in combined respiratory therapies, this inhaled treatment may facilitate increased access of therapeutic agents to bacteria and/or the lung cell surface. Mechanistic studies showed that this disruption of EPS structure was not simply related to interaction between OligoG CF-5/20 and the pseudomonal M-block alginate, but may rather reflect modification of QS signaling within the biofilm, as well as interactions with Ca^{2+}, DNA, and EPS. Work on elucidating these complex interactions is ongoing. The findings here, and the proven safety of the agent as an inhalational therapy (http://www.clinicaltrials.gov; identifiers NCT00970346 and NCT01465529), highlight the potential utility of the agent in the treatment of MDR bacterial infections in a range of human diseases. Phase IIb human studies are currently ongoing (http://www.clinicaltrials.gov; identifiers NCT02157922 and NCT02453789).

MATERIALS AND METHODS

Bacterial strains and media. *P. aeruginosa* strains were cultured on blood agar plates and grown overnight in tryptone soy broth (TSB) (LabM) at 37°C. MH medium or AS medium (adapted from earlier studies [42] by supplementation with 20 ml/liter RPMI 1640 as an amino acid source; Sigma-Aldrich) were also employed.

Reference strains ($n = 7$) were obtained from the IPARP (57), including AA2 and AA44 (early and late nonmucoid CF colonizers, respectively), AA43 (a late mucoidal colonizer from the same clonal origin), and mucoidal CF isolates IST 27 (Lisbon, Portugal) and 2192 (source ID, Boston, MA). The well-characterized nonmucoid PAO1 and mucoidal MDR CF strain NH57388A (Copenhagen, Denmark) were also used in subsequent experiments.

Patients and clinical isolates. Newly isolated nonmucoid *P. aeruginosa* strains (22078, 22554, and 22476) were obtained from induced sputa collected from children attending the Cystic Fibrosis Unit at the University Hospital of Wales, Cardiff, United Kingdom, participating in the Sputum Induction Trial (SpIT) study (a longitudinal sputum collection study in CF patients; Local Research Ethics Committee approved [project ID 11/RPM/5216]).

Changes in antibiotic susceptibility in different media. Bactericidal values for colistin in MH and AS media were studied using standard MIC assays as previously described (29).

Effects of OligoG CF-5/20 on pseudomonal growth in the presence of colistin. For the inoculum for the pseudomonal growth curves, overnight cultures in TSB ($n = 3$) were standardized to 10^6 cells/ml in MH medium. For treated samples, *P. aeruginosa* cultures (NH57388A; $n = 3$) standardized to 10^8 cells/ml in MH medium were treated with and without 2% OligoG CF-5/20 (wt/vol) with or without colistin (0.5× MIC; 0.05 μg/ml). Samples were grown (24 h; 37°C) in 96-well plates, and changes in cell density (optical density at 600 nm [OD_{600}]) were recorded every hour on a Fluostar Omega plate reader. The cell doubling time was calculated for each growth curve.

Viable-microbial-cell numbers in culture when treated with OligoG CF-5/20. ATP production levels by PAO1 and NH57388A were compared in MH and AS media with or without 2% OligoG CF-5/10. Cultures were prepared as for the growth curve experiments and analyzed using the BacTiter-Glo microbial cell viability assay (Promega) at 0, 2, 4, 6, 8, 12, 24, and 48 h, with luminescence read on a Fluostar Omega plate reader.

Confocal laser scanning microscopy of biofilms in MH and AS media in the presence of OligoG CF-5/20. Pseudomonal cultures (NH57388A) standardized to 10^7 CFU/ml were inoculated 1:20 in MH or AS medium and incubated (37°C; 20 rpm) for 24 h or 48 h, respectively, in Greiner glass bottom optical 96-well plates, with the difference in growth rates in the two media accounting for the longer growth time used for AS medium. For antimicrobial treatment, half of the supernatant was gently removed and replaced with fresh MH or AS medium with or without 2% OligoG CF-5/20 and/or colistin at half the MBEC (2 μg/ml) and incubated for 1 h. The supernatant was then removed and replaced with 6% (vol/vol) LIVE/DEAD (Invitrogen) stain in phosphate-buffered saline (PBS) prior to imaging. CLSM was performed using a Leica SP5 confocal microscope with ×63 magnification under oil; z-stack CLSM images were analyzed using COMSTAT image analysis software (33).

AS medium biofilms were also fixed overnight at 4°C with 3% (vol/vol) glutaraldehyde and stained (1 h) at room temperature with 0.15% Syto-9 (Invitrogen) in PBS. CLSM of z-stack images was achieved using sequential fluorescence recordings of Syto-9 ($\lambda_{ex}/\lambda_{em}$ maximum, 480 nm/500 nm) and propidium iodide ($\lambda_{ex}/\lambda_{em}$ maximum, 490 nm/635 nm).

For EPS imaging, NH57388A biofilms (48 h) were grown in AS medium in 12-well glass bottom plates (no. 1.5; MatTek Corp., Ashland, MA, USA) ± 2% or 6% OligoG CF-5/20. The biofilms were fixed with 2.5% glutaraldehyde in PBS overnight at 4°C. The fixative was then removed, and the biofilms were stained with Syto-9 (0.15% in PBS) and concanavalin A, Alexa Fluor 633 conjugate (100 μg/ml in PBS; Invitrogen), prior to CLSM imaging.

Scanning electron microscopy of OligoG CF-5/20-treated biofilms in different media. *P. aeruginosa* (PAO1 and NH57388A) cultures were adjusted to 10^7 CFU/ml in MH or AS medium and grown (37°C for 24 h or 48 h, respectively, at 20 rpm) in 12-well plates (Greiner Bio-One) on Thermanox glass slides (Agar Scientific) with or without 0.2%, 2%, or 6% (wt/vol) OligoG CF-5/20. For the established (24-h) biofilm model, half the supernatant was gently removed and replaced with 2% (vol/vol) OligoG CF-5/20, colistin (4× MBEC; 16 μg/ml), or a combination treatment and incubated for 24 h. The supernatant was removed, and the biofilms were fixed with 2.5% (vol/vol) glutaraldehyde prior to being washed (4 times) with distilled water (dH_2O) and freeze-dried. The samples were then gold coated and imaged using a Tescan Vega conventional scanning electron microscope (2.5 kV) for untreated samples and the established biofilm model or using a Hitachi S4800 (1-kV) scanning electron microscope for the biofilm development model. Pseudocoloring of SEM images was performed using Adobe Photoshop CS6 (Adobe Systems Europe Ltd., Maidenhead, United Kingdom). ImageJ was used to measure the microcolony diameter following line calibration using the known set scale for each image. Measurements of the three largest cellular aggregates in each image ($n \geq 42$/image) were taken at the narrowest diameter.

Direct interaction of OligoG CF-5/20 and pseudomonal high-molecular-weight alginate using circular dichroism spectroscopy. CD spectra of OligoG CF-5/20, high-mass alginate (approximately 100 kDa) comprising 7% guluronic acid derived from *P. aeruginosa*, and mixtures thereof were recorded using an Aviv model 215 instrument (Aviv Biomedical, Lakewood, NJ, USA). Samples were dissolved in 100 mM NaCl, 5 mM Tris-Cl, pH 7.5, and spun at 14,000 × *g* for 30 min at 4°C, and the supernatant was transferred to a 0.1-cm quartz cell prewarmed to 37°C. Repetitive spectra were collected from 245 to 196 nm at 0.2-nm intervals with 2-s accumulation per point (corresponding to ~11 min/spectrum). Buffer baselines were subtracted, and ellipticities (Θ) were corrected for dilutions.

Changes in quorum-sensing AHL production in different media when treated with OligoG CF-5/20. Overnight cultures of *P. aeruginosa* PAO1 were diluted (1:100) in either MH or AS medium and grown for a further 30 or 48 h ± 0.2% or 2% OligoG CF-5/20. The cultures were washed (3 times; 18,000 × *g*; 20 min; 4°C) in ice-cold 0.9% NaCl, and pelleted cells were dried (80°C) for 24 h and weighed. The culture supernatants were vigorously mixed (30 s) in equal volumes of ethyl acetate (acidified with 0.5% formic acid), and the upper layer was collected (3 times). The resultant ethyl acetate fractions were allowed to evaporate, and the precipitate was resuspended in 1 ml of distilled H_2O (58). Samples were freeze-dried prior to analysis. Quantification of acyl homoserine lactones was done using high-performance liquid chromatography (HPLC) triple-quadrupole mass spectrometry (LC-QQQ-MS). In each case, differences in culture biomass (at OligoG CF-5/20 concentrations of >2%) from cell-free culture supernatants used for the screening of AHLs was corrected by normalization according to dry weight.

Freeze-dried samples were maintained on ice and reconstituted in acetonitrile (200 μl) with 0.1% acetic acid and 7.2 ng ml^{-1} of the internal standard umbelliferone. Samples were centrifuged (16,100 × *g*; 10 min; 4°C), and the supernatants were filtered (0.4 μm; 2 times). Samples (5 μl) were loaded onto a C_{18} XDB Eclipse reverse-phase column (1.8 μm; 4.6 by 50 mm) and quantified using a 1200 series HPLC instrument coupled to a 6410B enhanced-sensitivity QQQ mass spectrometer (Agilent Technologies, Palo Alto, CA, USA). For detection using positive-ion mode, mobile phases A, comprised of 5 mM ammonium acetate in water modified with 0.1% acetic acid, and B, acetonitrile containing 0.1% acetic acid, were used. The column was equilibrated in 2% B before increasing in a linear fashion to 100% over 6 min; 100% B was maintained for a further 2 min before column reequilibration. The column temperature was maintained at 35°C for the duration, with a flow rate of 0.3 ml/min. Source parameters were set as follows: temperature, 350°C; gas flow, 10 liters/min; nebulizer, 35 lb/in^2; and capillary voltage, 4 kV. Data were analyzed using Agilent MassHunter QQQ quantitative analysis software (version B.07.00). Peak areas were normalized to the internal standard umbelliferone, and concentrations were calculated using standard concentration curves offset against blank values (the average peak areas for the blanks).

Statistical analysis. The COMSTAT data were normally distributed, so a standard *t* test was performed using MiniTab 17 (Minitab Ltd., Coventry, United Kingdom) with a Bonferroni correction. One-way analysis of variance (ANOVA) was performed for the AHL data using GraphPad 3 (GraphPad, La Jolla, CA, USA). STATA was used to carry out a Kruskal-Wallis nonparametric test supplemented by Dunn's test for the microcolony SEM measurements.

SUPPLEMENTAL MATERIAL

Supplemental material for this article may be found at https://doi.org/10.1128/AAC.00762-17.

SUPPLEMENTAL FILE 1, PDF file, 0.5 MB.
SUPPLEMENTAL FILE 2, MPG file, 13.4 MB.
SUPPLEMENTAL FILE 3, MPG file, 13.2 MB.

ACKNOWLEDGMENTS

This study was supported by funding from the European Union via the Eurostars Programme and the European Social Fund, Research Council of Norway, Cystic Fibrosis Foundation US, and AlgiPharma AS.

We thank N. Høiby for *P. aeruginosa* strain NH57388A, E. Mahenthiralingam for the IPARP strains, and Debbie Salmon for technical support for the LC-MS. We thank Gudmund Skjåk-Bræk for providing the high-M_w pseudomonal alginate for the CD studies. We also thank Damian Farnell for his support with statistical analysis.

D.W.T. has a consultancy relationship with and, along with K.E.H., has received research funding from AlgiPharma AS. A.D. and P.D.R. are director/owners of AlgiPharma AS. We have no other conflicts of interest to disclose.

REFERENCES

1. Valderrey AD, Pozuelo MJ, Jimenez PA, Macia MD, Oliver A, Rotger R. 2010. Chronic colonization by *Pseudomonas aeruginosa* of patients with obstructive lung diseases: cystic fibrosis, bronchiectasis, and chronic obstructive pulmonary disease. Diagn Microbiol Infect Dis 68:20–27. https://doi.org/10.1016/j.diagmicrobio.2010.04.008.
2. Farrell PM. 2008. The prevalence of cystic fibrosis in the European Union. J Cyst Fibros 7:450–453. https://doi.org/10.1016/j.jcf.2008.03.007.
3. Rubin BK. 2009. Mucus, phlegm, and sputum in cystic fibrosis. Respir Care 54:726–732.
4. Li ZH, Kosorok MR, Farrell PM, Laxova A, West SEH, Green CG, Collins J, Rock MJ, Splaingard ML. 2005. Longitudinal development of mucoid *Pseudomonas aeruginosa* infection and lung disease progression in children with cystic fibrosis. JAMA 293:581–588. https://doi.org/10.1001/jama.293.5.581.
5. Marvig RL, Johansen HK, Molin S, Jelsbak L. 2013. Genome analysis of a transmissible lineage of *Pseudomonas aeruginosa* reveals pathoadaptive mutations and distinct evolutionary paths of hypermutators. Plos Genet 9:e1003741. https://doi.org/10.1371/journal.pgen.1003741.
6. Feliziani S, Marvig RL, Lujan AM, Moyano AJ, Di Rienzo JA, Johansen HK, Molin S, Smania AM. 2014. Coexistence and within-host evolution of diversified lineages of hypermutable *Pseudomonas aeruginosa* in long-term cystic fibrosis infections. Plos Genet 10:e1004651. https://doi.org/10.1371/journal.pgen.1004651.
7. Marvig RL, Sommer LM, Molin S, Johansen HK. 2015. Convergent evolution and adaptation of *Pseudomonas aeruginosa* within patients with cystic fibrosis. Nat Genet 47:57–64. https://doi.org/10.1038/ng.3148.
8. Bales PM, Renke EM, May SL, Shen Y, Nelson DC. 2013. Purification and characterization of biofilm-associated EPS exopolysaccharides from ESKAPE organisms and other pathogens. PLoS One 8:e67950. https://doi.org/10.1371/journal.pone.0067950.
9. Ryall B, Carrara M, Zlosnik JEA, Behrends V, Lee X, Wong Z, Lougheed KE, Williams HD. 2014. The mucoid switch in *Pseudomonas aeruginosa* represses quorum sensing systems and leads to complex changes to stationary phase virulence factor regulation. PLoS One 9:e96166. https://doi.org/10.1371/journal.pone.0096166.
10. Ryall B, Davies JC, Wilson R, Shoemark A, Williams HD. 2008. *Pseudomonas aeruginosa*, cyanide accumulation and lung function in CF and non-CF bronchiectasis patients. Eur Respir J 32:740–747. https://doi.org/10.1183/09031936.00159607.
11. Leid JG, Willson CJ, Shirtliff ME, Hassett DJ, Parsek MR, Jeffers AK. 2005. The exopolysaccharide alginate protects *Pseudomonas aeruginosa* biofilm bacteria from IFN-gamma-mediated macrophage killing. J Immunol 175:7512–7518. https://doi.org/10.4049/jimmunol.175.11.7512.
12. Waine DJ, Honeybourne D, Smith EG, Whitehouse JL, Dowson CG. 2008. Association between hypermutator phenotype, clinical variables, mucoid phenotype, and antimicrobial resistance in *Pseudomonas aeruginosa*. J Clin Microbiol 46:3491–3493. https://doi.org/10.1128/JCM.00357-08.
13. Anonymous. 2014. Cystic fibrosis patient registry annual report. Cystic Fibrosis Foundation, Bethesda, MD. https://www.cff.org/Our-Research/CF-Patient-Registry/2015-Patient-Registry-Annual-Data-Report.pdf. Retrieved 19 July 2017.
14. Worlitzsch D, Tarran R, Ulrich M, Schwab U, Cekici A, Meyer KC, Birrer P, Bellon G, Berger J, Weiss T, Botzenhart K, Yankaskas JR, Randell S, Boucher RC, Doring G. 2002. Effects of reduced mucus oxygen concentration in airway *Pseudomonas* infections of cystic fibrosis patients. J Clin Invest 109:317–325. https://doi.org/10.1172/JCI0213870.
15. Kirchner S, Fothergill JL, Wright EA, James CE, Mowat E, Winstanley C. 5 June 2012. Use of artificial sputum medium to test antibiotic efficacy against *Pseudomonas aeruginosa* in conditions more relevant to the cystic fibrosis lung. J Vis Exp https://doi.org/10.3791/3857.
16. Fung C, Naughton S, Turnbull L, Tingpej P, Rose B, Arthur J, Hu H, Harmer C, Harbour C, Hassett DJ, Whitchurch CB, Manos J. 2010. Gene expression of *Pseudomonas aeruginosa* in a mucin-containing synthetic growth medium mimicking cystic fibrosis lung sputum. J Med Microbiol 59:1089–1100. https://doi.org/10.1099/jmm.0.019984-0.
17. Quinn RA, Whiteson K, Lim Y-W, Salamon P, Bailey B, Mienardi S, Sanchez SE, Blake D, Conrad D, Rohwer F. 2015. A Winogradsky-based culture system shows an association between microbial fermentation and cystic fibrosis exacerbation. ISME J 9:1024–1038. https://doi.org/10.1038/ismej.2014.234.
18. McCarthy RR, Mooij MJ, Reen FJ, Lesouhaitier O, O'Gara F. 2014. A new regulator of pathogenicity (bvlR) is required for full virulence and tight microcolony formation in *Pseudomonas aeruginosa*. Microbiology 160:1488–1500. https://doi.org/10.1099/mic.0.075291-0.
19. Windmüller N, Witten A, Block D, Bunk B, Sproeer C, Kahl BC, Mellmann A. 2015. Transcriptional adaptations during long-term persistence of *Staphylococcus aureus* in the airways of a cystic fibrosis patient. Int J Med Microbiol 305:38–46. https://doi.org/10.1016/j.ijmm.2014.10.005.
20. Nafee N, Husari A, Maurer CK, Lu C, de Rossi C, Steinbach A, Hartmann RW, Lehr C-M, Schneider M. 2014. Antibiotic-free nanotherapeutics: Ultra-small, mucus-penetrating solid lipid nanoparticles enhance the pulmonary delivery and anti-virulence efficacy of novel quorum sensing inhibitors. J Control Release 192:131–140. https://doi.org/10.1016/j.jconrel.2014.06.055.
21. Yang Y, Tsifansky MD, Wu CJ, Yang HI, Schmidt G, Yeo Y. 2010. Inhalable antibiotic delivery using a dry powder co-delivering recombinant deoxyribonuclease and ciprofloxacin for treatment of cystic fibrosis. Pharm Res 27:151–160. https://doi.org/10.1007/s11095-009-9991-2.
22. Nguyen D, Joshi-Datar A, Lepine F, Bauerle E, Olakanmi O, Beer K, McKay G, Siehnel R, Schafhauser J, Wang Y, Britigan BE, Singh PK. 2011. Active starvation responses mediate antibiotic tolerance in biofilms and nutrient-limited bacteria. Science 334:982–986. https://doi.org/10.1126/science.1211037.
23. Filkins LM, O'Toole GA. 2015. Cystic fibrosis lung infections: polymicrobial, complex, and hard to treat. Plos Pathog 11:e1005258. https://doi.org/10.1371/journal.ppat.1005258.
24. Barry PJ, Jones AM. 2015. New and emerging treatments for cystic fibrosis. Drugs 75:1165–1175. https://doi.org/10.1007/s40265-015-0424-8.
25. Li J, Nation RL, Turnidge JD, Milne RW, Coulthard K, Rayner CR, Paterson DL. 2006. Colistin: the re-emerging antibiotic for multidrug-resistant Gram-negative bacterial infections. Lancet Infect Dis 6:589–601. https://doi.org/10.1016/S1473-3099(06)70580-1.
26. Azzopardi EA, Ferguson EL, Thomas DW. 2013. The enhanced permeability retention effect: a new paradigm for drug targeting in infection. J Antimicrob Chemother 68:257–274. https://doi.org/10.1093/jac/dks379.
27. Li J, Nation RL, Milne RW, Turnidge JD, Coulthard K. 2005. Evaluation of colistin as an agent against multi-resistant in Gram-negative bacteria. Int J Antimicrob Agents 25:11–25. https://doi.org/10.1016/j.ijantimicag.2004.10.001.

28. Barriere SL. 2015. Clinical, economic and societal impact of antibiotic resistance. Expert Opin Pharmacother 16:151–153. https://doi.org/10.1517/14656566.2015.983077.
29. Khan S, Tondervik A, Sletta H, Klinkenberg G, Emanuel C, Onsøyen E, Myrvold R, Howe RA, Walsh TR, Hill KE, Thomas DW. 2012. Overcoming drug resistance with alginate oligosaccharides able to potentiate the action of selected antibiotics. Antimicrob Agents Chemother 56:5134–5141. https://doi.org/10.1128/AAC.00525-12.
30. Powell LC, Pritchard MF, Emanuel C, Onsøyen E, Rye PD, Wright CJ, Hill KE, Thomas DW. 2014. A nanoscale characterization of the interaction of a novel alginate oligomer with the cell surface and motility of *Pseudomonas aeruginosa*. Am J Respir Cell Mol Biol 50:483–492. https://doi.org/10.1165/rcmb.2013-0287OC.
31. Pritchard MF, Powell LC, Menzies GE, Lewis PD, Hawkins K, Wright C, Doull I, Walsh TR, Onsøyen E, Dessen A, Myrvold R, Rye PD, Myrset AH, Stevens HNE, Hodges LA, MacGregor G, Neilly JB, Hill KE, Thomas DW. 2016. A new class of safe oligosaccharide polymer therapy to modify the mucus barrier of chronic respiratory disease. Mol Pharm 13:863–872. https://doi.org/10.1021/acs.molpharmaceut.5b00794.
32. Hengzhuang W, Song Z, Ciofu O, Onsøyen E, Rye PD, Høiby N. 2016. OligoG CF-5/20 disruption of mucoid *Pseudomonas aeruginosa* biofilm in a murine lung infection model. Antimicrob Agents Chemother 60:2620–2626. https://doi.org/10.1128/AAC.01721-15.
33. Heydorn A, Nielsen AT, Hentzer M, Sternberg C, Givskov M, Ersboll BK, Molin S. 2000. Quantification of biofilm structures by the novel computer program COMSTAT. Microbiology 146:2395–2407. https://doi.org/10.1099/00221287-146-10-2395.
34. Morris ER, Rees DA, Sanderson GR, Thom D. 1975. Conformation and circular dichroism of uronic acid residues in glycosides and polysaccharides. J Chem Soc Perk 2:1418–1425. https://doi.org/10.1039/p29750001418.
35. Ciofu O, Tolker-Nielsen T, Jensen PO, Wang H, Høiby N. 2015. Antimicrobial resistance, respiratory tract infections and role of biofilms in lung infections in cystic fibrosis patients. Adv Drug Deliv Rev 85:7–23. https://doi.org/10.1016/j.addr.2014.11.017.
36. Sherrard LJ, Tunney MM, Elborn JS. 2014. Antimicrobial resistance in the respiratory microbiota of people with cystic fibrosis. Lancet 384:703–713. https://doi.org/10.1016/S0140-6736(14)61137-5.
37. Ceri H, Olson ME, Stremick C, Read RR, Morck D, Buret A. 1999. The Calgary biofilm device: new technology for rapid determination of antibiotic susceptibilities of bacterial biofilms. J Clin Microbiol 37:1771–1776.
38. Liu Y-Y, Wang Y, Walsh TR, Yi L-X, Zhang R, Spencer J, Doi Y, Tian G, Dong B, Huang X, Yu L-F, Gu D, Ren H, Chen X, Lv L, He D, Zhou H, Liang Z, Liu J-H, Shen J. 2016. Emergence of plasmid-mediated colistin resistance mechanism MCR-1 in animals and human beings in China: a microbiological and molecular biological study. Lancet Infect Dis 16:161–168. https://doi.org/10.1016/S1473-3099(15)00424-7.
39. Breidenstein EBM, de la Fuente-Nunez C, Hancock REW. 2011. *Pseudomonas aeruginosa*: all roads lead to resistance. Trends Microbiol 19:419–426. https://doi.org/10.1016/j.tim.2011.04.005.
40. Nation RL, Li J, Cars O, Couet W, Dudley MN, Kaye KS, Mouton JW, Paterson DL, Tam VH, Theuretzbacher U, Tsuji BT, Turnidge JD. 2015. Framework for optimisation of the clinical use of colistin and polymyxin B: the Prato polymyxin consensus. Lancet Infect Dis 15:225–234. https://doi.org/10.1016/S1473-3099(14)70850-3.
41. Huang JX, Blaskovich MAT, Pelingon R, Ramu S, Kavanagh A, Elliott AG, Butler MS, Montgomery AB, Cooper MA. 2015. Mucin binding reduces colistin antimicrobial activity. Antimicrob Agents Chemother 59:5925–5931. https://doi.org/10.1128/AAC.00808-15.
42. Sriramulu DD, Lunsdorf H, Lam JS, Romling U. 2005. Microcolony formation: a novel biofilm model of *Pseudomonas aeruginosa* for the cystic fibrosis lung. J Med Microbiol 54:667–676. https://doi.org/10.1099/jmm.0.45969-0.
43. Nivens DE, Ohman DE, Williams J, Franklin MJ. 2001. Role of alginate and its O acetylation in formation of *Pseudomonas aeruginosa* microcolonies and biofilms. J Bacteriol 183:1047–1057. https://doi.org/10.1128/JB.183.3.1047-1057.2001.
44. Garnett JA, Matthews S. 2012. Interactions in bacterial biofilm development: a structural perspective. Curr Protein Pept Sci 13:739–755. https://doi.org/10.2174/138920312804871166.
45. Billings N, Millan MR, Caldara M, Rusconi R, Tarasova Y, Stocker R, Ribbeck K. 2013. The extracellular matrix component Psl provides fast-acting antibiotic defense in *Pseudomonas aeruginosa* biofilms. PLoS Pathog 9:e1003526. https://doi.org/10.1371/journal.ppat.1003526.
46. Diaz Caballero JD, Clark ST, Coburn B, Zhang Y, Wang PW, Donaldson SL, Tullis DE, Yau YCW, Waters VJ, Hwang DM, Guttman DS. 2015. Selective sweeps and parallel pathoadaptation drive *Pseudomonas aeruginosa* evolution in the cystic fibrosis lung. mBio 6:e00981-15. https://doi.org/10.1128/mBio.00981-15.
47. Carroll SM, Lee M-C, Marx CJ. 2014. Sign epistasis limits evolutionary trade-offs at the confluence of single- and multi-carbon metabolism in *Methylobacterium extorquens* AM1. Evolution 68:760–771. https://doi.org/10.1111/evo.12301.
48. Jiang P, Li J, Han F, Duan G, Lu X, Gu Y, Yu W. 2011. Antibiofilm antibiofilm activity of an exopolysaccharide from marine bacterium *Vibrio* sp QY101. PLoS One 6:e18514. https://doi.org/10.1371/journal.pone.0018514.
49. Alipour M, Suntres ZE, Omri A. 2009. Importance of DNase and alginate lyase for enhancing free and liposome encapsulated aminoglycoside activity against *Pseudomonas aeruginosa*. J Antimicrob Chemother 64:317–325. https://doi.org/10.1093/jac/dkp165.
50. Alkawash MA, Soothill JS, Schiller NL. 2006. Alginate lyase enhances antibiotic killing of mucoid *Pseudomonas aeruginosa* in biofilms. APMIS 114:131–138. https://doi.org/10.1111/j.1600-0463.2006.apm_356.x.
51. Lembre P, Lorentz CC, Di Martino P. 2012. Exopolysaccharides of the biofilm matrix: a complex biophysical world. INTECH Open Access Publisher, Rijeka, Croatia. http://www.intechopen.com/books/the-complex-world-of-polysaccharides/exopolysaccharides-of-the-biofilm-matrix-a-complex-biophysical-world.
52. Flemming HC, Wingender J. 2010. The biofilm matrix. Nat Rev Microbiol 8:623–633. https://doi.org/10.1038/nrmicro2415.
53. Sletmoen M, Maurstad G, Nordgård CT, Draget KI, Stokke BT. 2012. Oligoguluronate induced competitive displacement of mucin-alginate interactions: relevance for mucolytic function. Soft Matter 8:8413–8421.
54. Aslam SN, Newman MA, Erbs G, Morrissey KL, Chinchilla D, Boller T, Jensen TT, De Castro C, Ierano T, Molinaro A, Jackson RW, Knight MR, Cooper RM. 2008. Bacterial polysaccharides suppress induced innate immunity by calcium chelation. Curr Biol 18:1078–1083. https://doi.org/10.1016/j.cub.2008.06.061.
55. Martinez-Gomez F, Mansilla A, Matsuhiro B, Matulewicz MC, Troncoso-Valenzuela MA. 2016. Chiroptical characterization of homopolymeric block fractions in alginates. Carbohydr Polym 146:90–101. https://doi.org/10.1016/j.carbpol.2016.03.047.
56. Grant GT, Morris ER, Rees DA, Smith PJC, Thom D. 1973. Biological interactions between polysaccharides and divalent cations: the egg-box model. FEBS Lett 32:195–198. https://doi.org/10.1016/0014-5793(73)80770-7.
57. De Soyza A, Hall AJ, Mahenthiralingam E, Drevinek P, Kaca W, Drulis-Kawa Z, Stoitsova SR, Toth V, Coenye T, Zlosnik JEA, Burns JL, Sa-Correia I, De Vos D, Pirnay J-P, Kidd TJ, Reid D, Manos J, Klockgether J, Wiehlmann L, Tuemmler B, McClean S, Winstanley C, EU FP7 funded COST Action BM1003 "Cell surface virulence determinants of cystic fibrosis pathogens". 2013. Developing an international *Pseudomonas aeruginosa* reference panel. Microbiologyopen 2:1010–1023. https://doi.org/10.1002/mbo3.141.
58. Ravn L, Christensen AB, Molin S, Givskov M, Gram L. 2001. Methods for detecting acylated homoserine lactones produced by Gram-negative bacteria and their application in studies of AHL-production kinetics. J Microbiol Methods 44:239–251. https://doi.org/10.1016/S0167-7012(01)00217-2.